Y. W. Kwon
J. K. Bergersen
Y. S. Shin
Mechanical Engineering Department
Naval Postgraduate School
Monterey, CA 93943

Effect of Surface Coatings on Cylinders Exposed to Underwater Shock

The response of a coated cylinder (metallic cylinder coated with a rubber material) subjected to an underwater explosion is analyzed numerically. The dynamic response of the coated cylinder appears to be adversely affected when impacted by an underwater shock wave under certain conditions of geometry and material properties of the coating. When adversely affected, significant deviations in values of axial stress, hoop stress, and strain are observed. The coated cylinder exhibits a larger deformation and higher internal energy in the metallic material. Rubber coatings appeared to inhibit energy dissipation from the metallic material to the surrounding water medium. A parametric study of various coatings was performed on both aluminum and steel cylinders. The adverse effect of the coating decreased when the stiffness of the rubber layer increased, indicating the existence of a threshold value. The results of this study indicate that the stiffness of the coating is a critical factor to the shock hardening of the coated cylinder. © *1994 John Wiley & Sons, Inc.*

INTRODUCTION

The dynamic response of a structure to an underwater explosion is a complex problem due to the interaction between the fluid and structure. In the past, extensive research was conducted in the field of underwater shock to better understand the effects of blast damage on shock hardening of a structure. The study has involved both physical testing and numerical modeling of uncoated metal cylinders of various configurations such as unstiffened, stiffened, single shell layer and double shell layer models. Ship shock qualifications and even small scale testing can be cost prohibitive and time consuming, therefore much of the work has focused on developing computer models using numerical analysis techniques. Results from earlier studies (Nelson, Shin, and Kwon, 1992; Fox, Kwon, and Shin, 1992; Chisum, 1992) indicate response predictions compare favorably with both analytical solutions and experimental data.

In a recent study, when subjected to an underwater shock wave, damage to a steel test panel increased when it was covered with a low density layer of glass microspheres suspended in water (slurry). An early work (Geers 1975) showed that resilient scatterers can attenuate the near-field pressure if they behave like a cavity-like boundary. Such an attenuation will certainly change the dynamic response of the structure.

The objective of this study was to examine the response of a metal cylinder coated with a rubber material, when subjected to an underwater explosion, utilizing a numerical analysis technique. Rubber coated aluminum and steel cylinders were analyzed and a parametric study of various coatings was performed to gain a better understanding of the coating effect on the structure.

Received November 25, 1992; Accepted August 19, 1993.
Shock and Vibration, Vol. 1, No. 3, pp. 253–265 (1994)

CCC 1070-9622/94/030253-13

NUMERICAL ANALYSIS

To study the effects of an underwater shock wave on a cylinder, coupled finite-element and boundary-element codes were utilized. The two codes operate in tandem so that the fluid–structure interaction can be calculated. These codes were successfully implemented and has since been the primary tool used for studying underwater shock phenomena (Fox et al., 1992). Structural calculations were handled by the finite element code and the fluid–structure interaction was handled by the boundary element code.

The finite element code used in this analysis was VEC/DYNA3D (Stillman and Hallquist, 1990). The code is efficient and flexible, offering a wide variety of material models. The boundary element method code used was USA (underwater shock analysis) (DeRuntz, 1989). Calculations of the fluid–structure interaction are based on the doubly asymptotic approximation (DAA) theory developed by Geers (1971, 1978). The boundary element method avoids the requirement to discretize the water medium. As a result, the number of degrees of freedom is much reduced.

Some fundamentals of the fluid–structure interaction are explained below. A detailed explanation is provided in DeRuntz (1989). The differential equation for the dynamic response of a structure can be expressed as follows:

$$[M_s]\{\ddot{x}\} + [C_s]\{\dot{x}\} + [K_s]\{x\} = \{f\} \qquad (1)$$

where $[M_s]$, $[C_s]$, and $[K_s]$ are the structural mass, damping, and stiffness matrices respectively, $\{x\}$ is the nodal displacement vector, and superimposed dot denotes a temporal derivative. $\{f\}$ is the excitation force vector and can be expressed as a function of the incident and scattered pressures of the impinging shock wave and any external loads applied to the dry surface of the structure. Their functional relationship is as follows:

$$\{f\} = -[G][A_f]\{P_i + P_s\} + \{f_d\} \qquad (2)$$

where $[G]$ is the fluid/structure transformation matrix, $[A_f]$ is the diagonal area matrix associated with the fluid elements, $\{P_i + P_s\}$ is the incident and scattered pressure wave vector and $\{f_d\}$ is the force vector applied to the dry surface. The incident pressure on the wet surface is known from the characteristics of an underwater explosion. However, the scattered pressure is unknown and it is computed from the fluid–structure interaction.

In order to determine the scattered pressure, the wave equation for the surrounding water medium must be solved. The surrounding medium is usually an infinite domain. In the context of finite element analysis, an infinite domain is modeled as a substantially large finite domain or as a rather small finite domain with infinite elements. Infinite elements approximate the nonreflection boundary of an infinite medium. In order to improve the approximation of the nonreflection boundary using infinite elements, the infinite elements need to be some distance away from the structure boundary. As a result, the number of finite elements to model the acoustic medium generally exceeds the number of structural elements. The conventional boundary element method needs a volume integration for the transient problem (Banerjee and Butterfield, 1981). This makes it necessary to discretize the domain of the water medium. All these techniques usually demand very expensive computation. The doubly asymptotic approximation, called DAA, makes the computation more efficient by completely avoiding any volume integration of the surrounding medium (Geers, 1971, 1978). DAA approaches to exactness at both early time and late time but not in between. A high-order DAA theory (Geers, 1978) was formulated to improve the accuracy of the first-order approximation. In the present study, the high-order DAA theory was used to solve for the scattered pressure because the high-order theory contains the first-order as a special case. DAA relates the scattering pressure to scattering wave particle velocity. The detail of both DAAs are explained in Geers (1971, 1978) so that it is not repeated here.

The scattering wave particle velocity is related to the structural response as shown below:

$$[G]^T\{\dot{x}\} = \{\dot{u}_i\} + \{\dot{u}_s\} \qquad (3)$$

where subscripts i and s denote incident and scattering velocities, respectively, and the incident wave particle velocity is known. As a result, the fluid–structure interaction can be solved using the previous equations. Those equations are coupled so that they have to be solved together. Instead of solving the equations simultaneously, the staggered time integration technique was used. In addition, augmentation was applied to the coupled equations in order to improve the

stability of time integration (Park, Felippa, and DeRuntz, 1977). As a result, the staggered solution procedure becomes unconditionally stable, at least for linear response of the structure.

DESCRIPTION OF MODEL

Material Description

The metal material was assumed to undergo the elastoplastic deformation. Two different metals were used. Aluminum was assumed to have no strain-rate hardening and steel was assumed to have strain-rate hardening. The Cowpers–Symonds model was used for the strain-rate hardening of the steel. The model is shown below:

$$\sigma_y = \sigma_y \left[1 + \left(\frac{\dot{\varepsilon}}{C}\right)^{1/p}\right] \tag{4}$$

where σ_y and ε is the yield stress and strain, and c and p are the strain-rate parameters. The material properties used in the present study are tabulated in Tables 1 and 2.

The behavior of the rubber material was based on the compressible Mooney–Rivlin model. Mooney (1940) pioneered a new approach to analyze the deformation of a soft material such as rubber. He stated that classical elastic theory could not be applied to a highly elastic (hyperelastic or superelastic) material but that deformation could be accurately represented in terms of its general strain energy density.

Mooney postulated that in addition to being homogeneous and free from hysteresis, a hyperelastic material possesses the following properties: It is isotropic in the undeformed state and remains isotropic in planes that are at right angles to a stretch or squeeze. Deformations are isometric, that is, occur without change in volume. In simple shear, shearing stress in any isotropic plane is proportional to the shear force.

Table 1. Aluminum (6061-T6) Properties

Density	5.412 slugs/ft^3
Poisson's ratio	0.33
Young's modulus	1.08×10^7 psi
Yield stress	4.0×10^4 psi
Speed of sound	16,400 ft/s

Table 2. Steel (ASTM A106 grade C) Properties

Density	15.218 slugs/ft^3
Poisson's ratio	0.30
Young's modulus	2.9×10^7 psi
Hardening modulus	1.114×10^5 psi
Yield stress	4.7×10^4 psi
Strain-rate parameter (c)	8.797×10^4/s
Strain-rate parameter (p)	5.65
Speed of sound	16,900 ft/s

Mooney expressed the general strain energy density function of a material, W, as follows:

$$W = \frac{G}{4}\sum_{i=1}^{3}\left(\lambda_i - \frac{1}{\lambda_i}\right)^2 + \frac{H}{4}\sum_{i=1}^{3}\left(\lambda_i^2 - \frac{1}{\lambda_i^2}\right) \tag{5}$$

where G and H represent the modulus of rigidity and the modulus characterizing asymmetry of reciprocal deformation, respectively. The variable H is a measure of the ability of a material to store energy when compressed as opposed to when stretched. λ_i is the principal stretch. To express the asymmetry of reciprocal deformation in a more useful form, Mooney defined a new parameter, called the coefficient of symmetry, as follows:

$$\alpha = \frac{H}{G}. \tag{6}$$

Two types of rubber, tread stock, and gum stock were considered. The material properties of the rubbers are shown in Table 3.

Geometric Description

All cases involved identical, numerical test conditions. The problem simulated detonation of 60 lbs of HBX-1 spherically shaped explosive at a horizontal standoff distance of 25 ft from the cylinder resulting in a side-on attack geometry. The uncoated cylinder models (metal only) were 12-in. diameter, 42-in. long, 0.25-in. thick (shell

Table 3. Rubber Properties

Density	1.908 slugs/ft^3
Speed of sound	100 ft/s
Shear modulus (tread)	95.8 psi
Coef. of asymmetry (tread)	0.223
Shear modulus (gum)	48.6 psi
Coef. of asymmetry (gum)	0.448

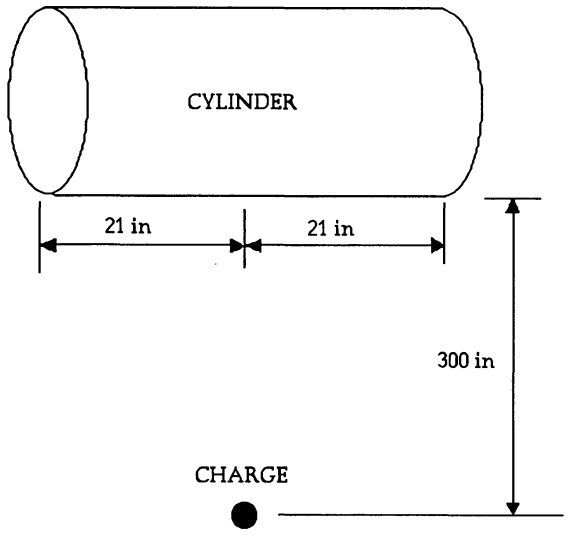

FIGURE 1 Cylinder geometry and test profile.

thickness) with a 1-in. thick endplate. The coated cylinder models had the same dimensions for the metal material as the uncoated cylinders but in addition were coated with 0.25 in. of rubber material on the outer surface of the cylinder. The shell and coating thicknesses were nominal values and were changed for parametric study. The cylinder geometry and the test profile are shown in Fig. 1. Actual pressure–time history data from a previous physical test for an uncoated aluminum cylinder (Fox et al., 1992) was utilized in the analysis. The pressure-time history plot is shown in Fig. 2.

The problem geometry involved two planes of symmetry that allowed the cylinder to be modeled as a quarter cylinder. Appropriate boundary constraints were applied along the symmetric planes. The finite element mesh for the quarter model is shown in Fig. 3. The metal material consisted of 186 solid-shell elements and the rubber material consisted of 198 solid elements. A total of nine locations were selected to compare stresses and strains in each case, three at the center section of the cylinder, three near the endplate, and three midway between the center section and the endplate. At each section the three locations were approximately equally spaced around the surface of the cylinder. A1 represents the element closest to the charge. The metal shell material in Fig. 3 shows the element orientation. Unless otherwise specified, all plots pertain to these element locations. Although the response of the rubber was examined in different cases, the analysis of the metal response was the primary objective. Therefore most of the results presented are for the metal material.

RESULTS AND DISCUSSION

The purpose of this study was to determine the effects of surface coatings on the dynamic re-

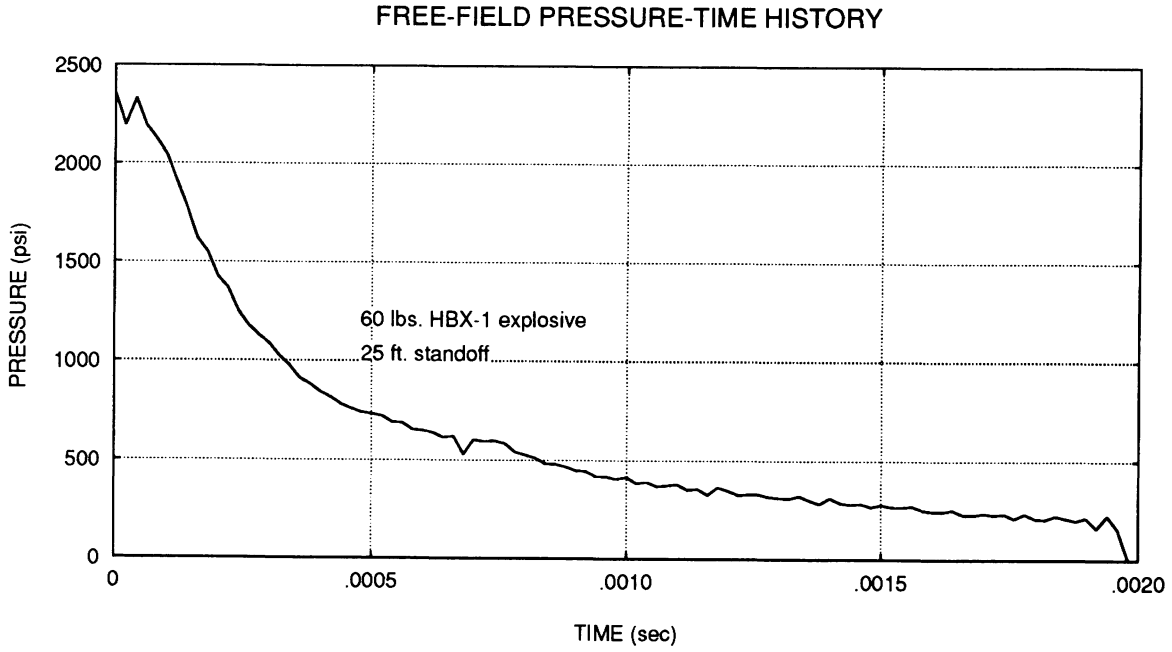

FIGURE 2 Free-field pressure-time history plot.

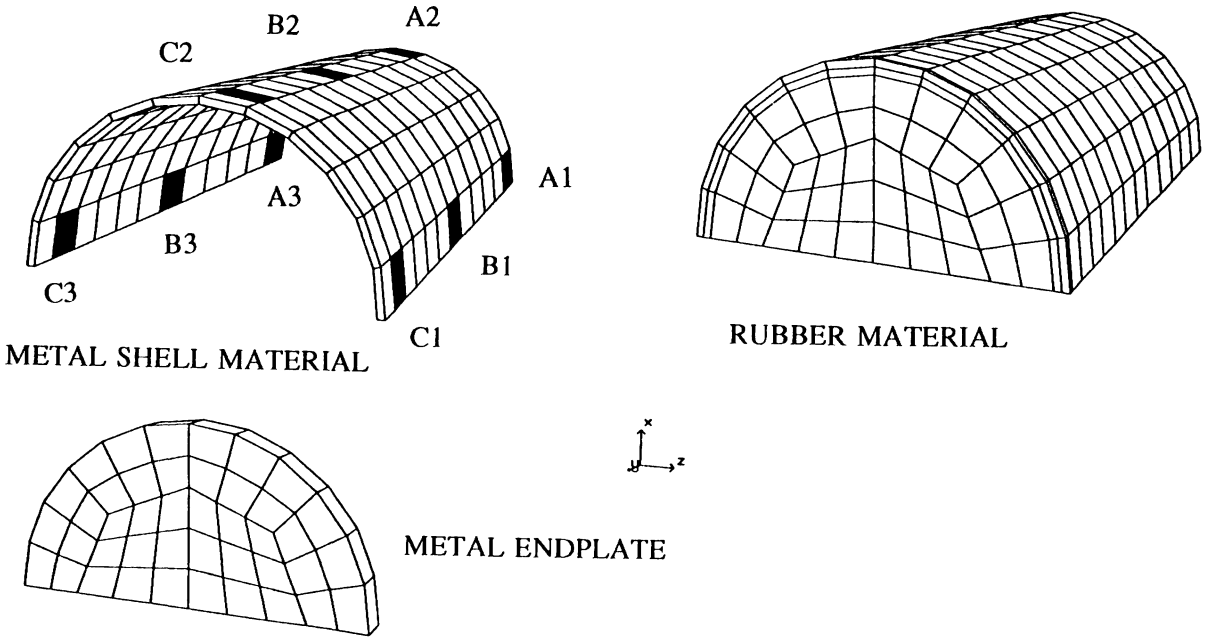

FIGURE 3 Finite element mesh of a quarter model.

sponse of cylinders subjected to underwater shock. A total of five cases were analyzed. In the first case, an uncoated aluminum cylinder was compared to two coated cylinders, one coated with tread stock rubber (referred to as composite model 1) and the other coated with gum stock rubber (referred to as composite model 2). The aluminum shell material and the rubber coating were both 0.250-in. thick. Both composite cylinders exhibited higher values of stress and strain than the uncoated cylinder at all the positions. For example, Fig. 4 and 5 are axial and hoop strains at the closest point from the charge, that is, position A1. In early time, (less than 1 ms) response was approximately the same between the uncoated and coated cylinders. (Passage of

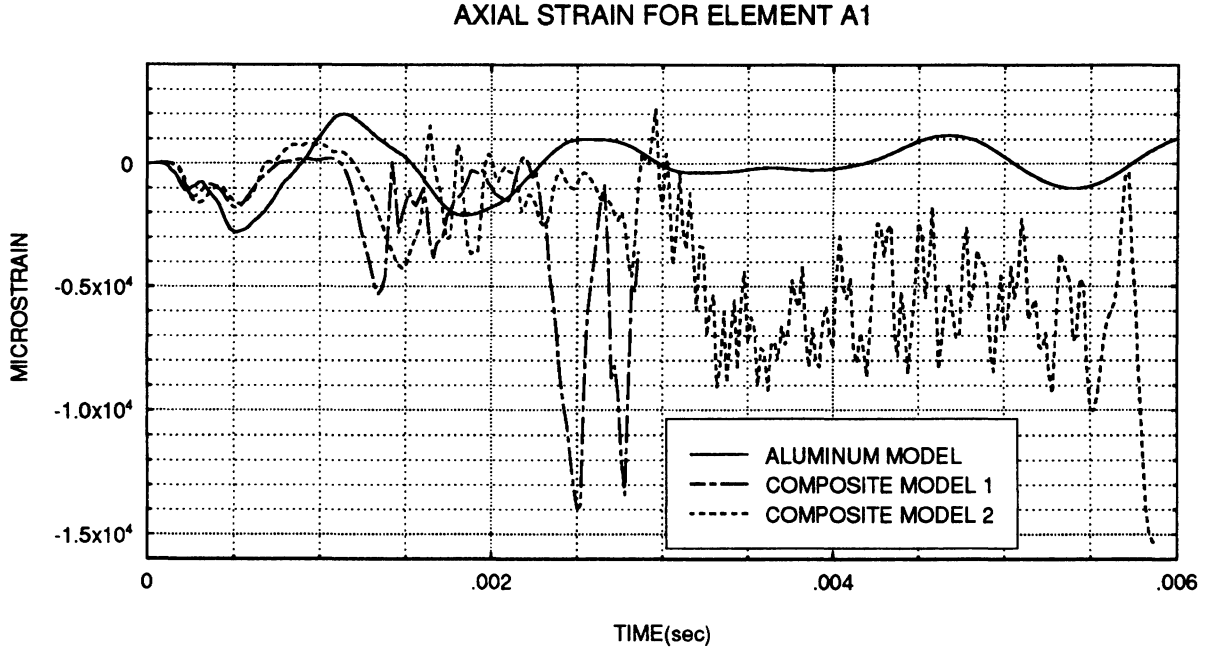

FIGURE 4 Axial strain at position A1 for uncoated and coated aluminum cylinders.

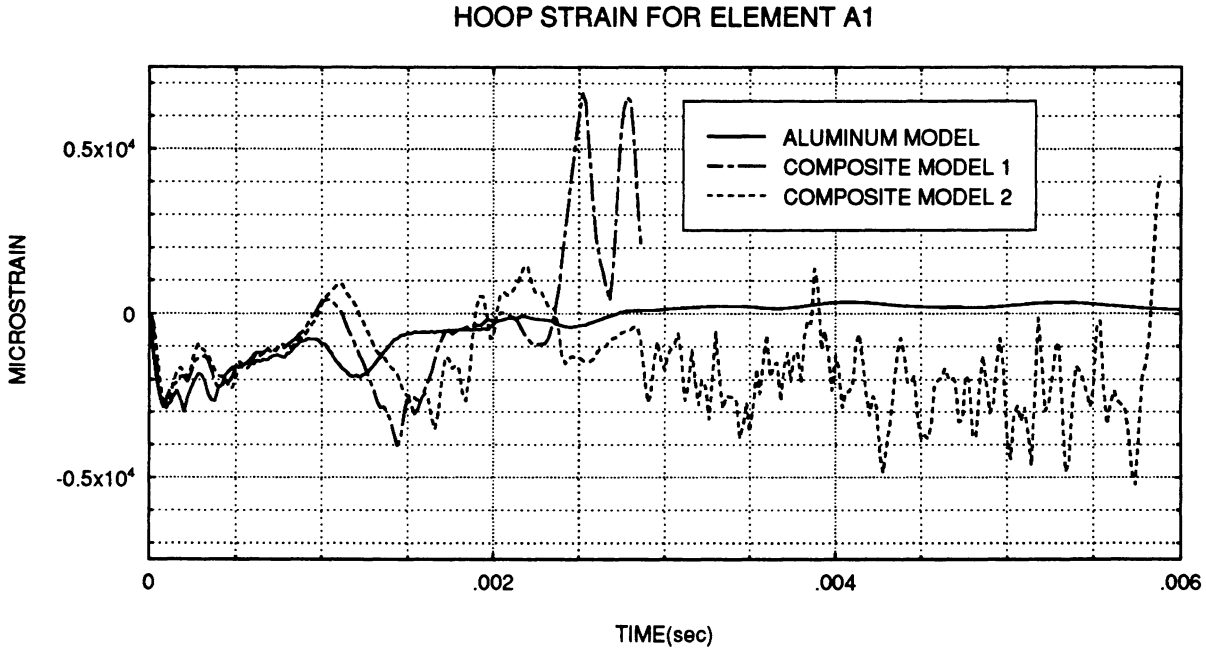

FIGURE 5 Hoop strain at position A1 for uncoated and coated aluminum cylinders.

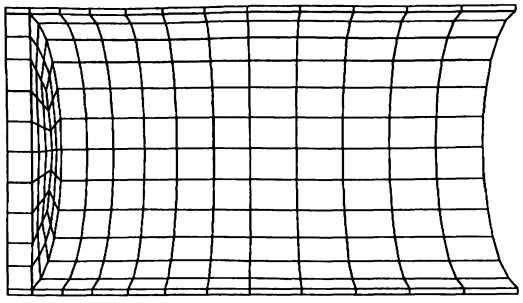

ALUMINUM MODEL

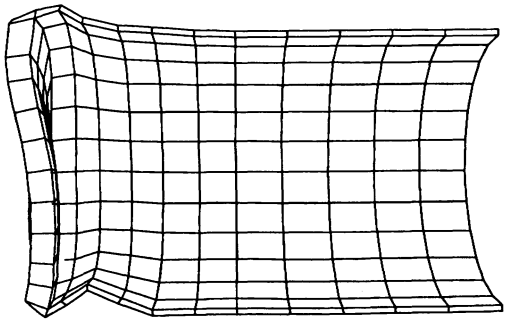

COMPOSITE MODEL 2

FIGURE 6 Deformation of uncoated and coated cylinders at 5.86 ms.

the shock wave occurred at about 0.2 ms) The deviations became significant after 1 ms. Neither composite cylinder showed consistently higher magnitudes than the other because this varied depending on the location analyzed. Both composite models exhibited higher oscillation than the uncoated model.

The results from this study indicate that the rubber coating tended to concentrate energy in the metal cylinder rather than allow for a rapid release of energy into the water medium, as in the uncoated case. The effects of the rubber coating are clearly visible in the deformation of the cylinders. Figure 6 shows deformation of the uncoated cylinder and the composite cylinder 2 at 5.86 ms. The high values of strain attained at locations near the endplate may be attributed to the inertial effects of the thick endplate. Figure 7 shows a comparison of the internal energy level in the aluminum shell material for the uncoated cylinder and the two coated cylinders, the latter exhibiting significantly higher values. The effects of the rubber coatings on the cylinder were significant and it seems that the adverse response of the coated cylinders is related to the energy build-up in the metallic material caused by the rubber coatings.

In the next phase of study, the analysis is focused on altering certain parameters to determine if they had any effect on cylinder response.

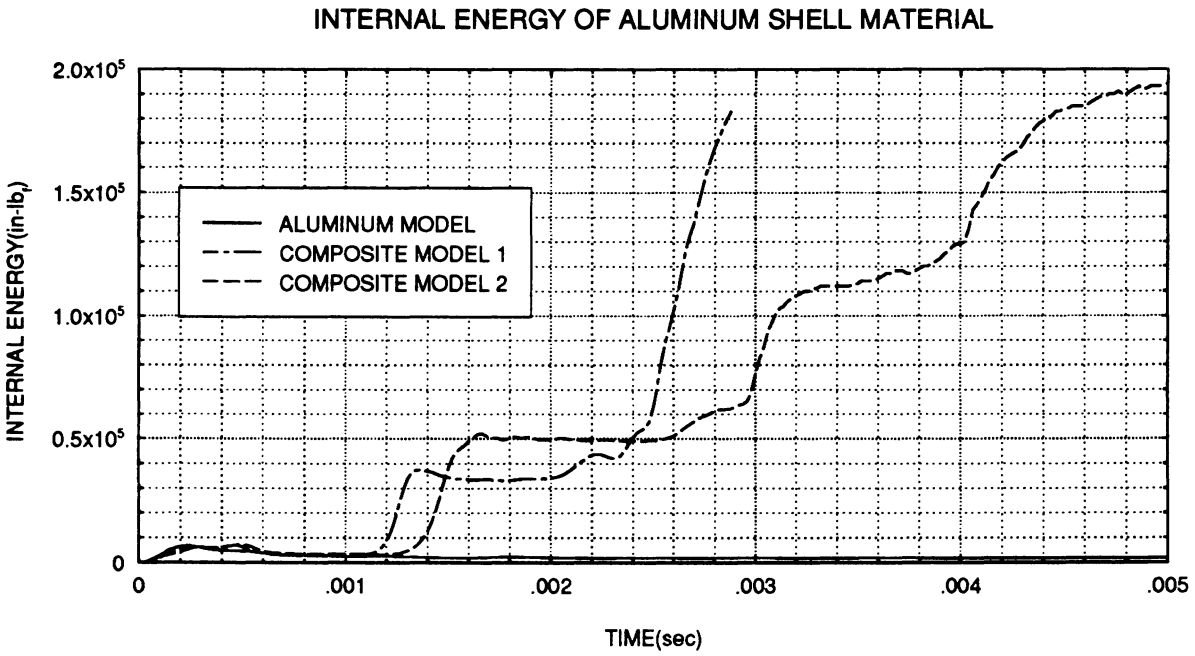

FIGURE 7 Internal energy of aluminum shell material for uncoated and coated cylinders.

In the first case, composite model 1 was used and the shear modulus of the rubber was increased with the coefficient of asymmetry held constant. As the modulus was increased by orders of magnitude, the response of the cylinder dramatically improved. Effective plastic strain is plotted for element A3, located at the backside at the center, and is shown in Fig. 8. For shear modulus values at or above 500 psi, the aluminum exhibited significantly lower strain. The high shear modulus was beneficial so that it reduced the plastic strains compared to that for the uncoated cylinder. To help visualize how the response was affected by a change in the material property of the

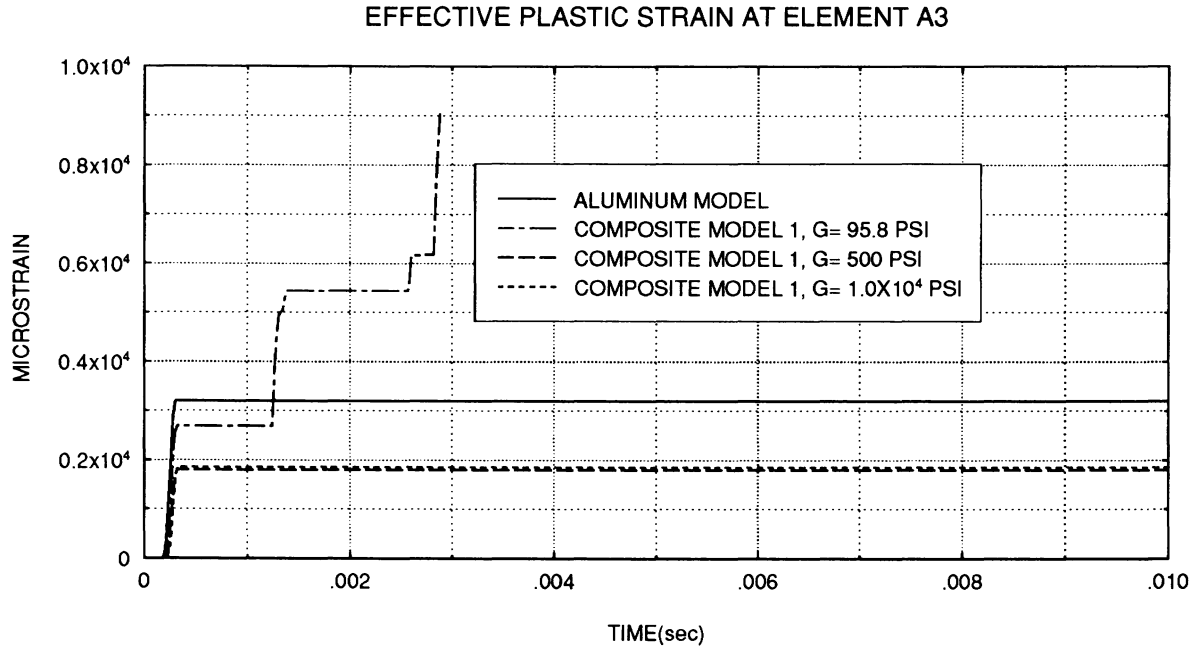

FIGURE 8 Effective plastic strain at position A3 for uncoated and coated cylinders with large variation of rubber shear modulus.

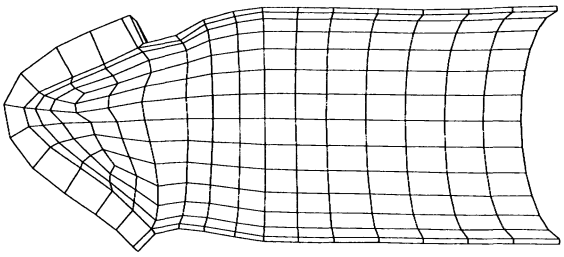

COMPOSITE MODEL 1 (G=95.8 PSI)

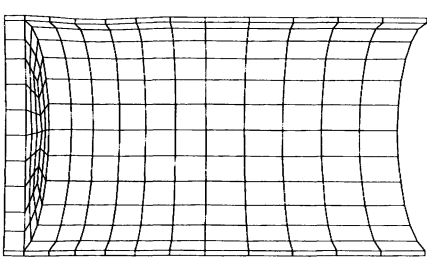

COMPOSITE MODEL 1 ($G=1X10^4$ PSI)

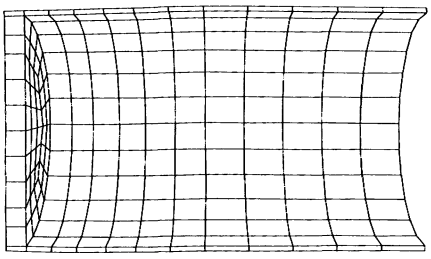

COMPOSITE MODEL 1 ($G=1X10^6$ PSI)

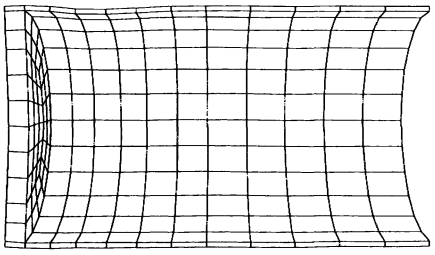

ALUMINUM MODEL

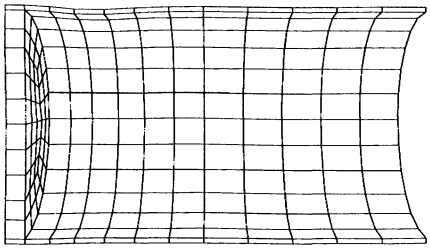

COMPOSITE MODEL 1 (G=500 PSI)

FIGURE 9 Deformation of uncoated and coated aluminum cylinders with large variation of rubber shear modulus at 2.86 ms.

rubber, radial velocity at the back of the cylinder center was examined. It is shown that at values at or above 500 psi, the velocity response is not erratic as in the low shear modulus case, but rather shows a gradual and smooth return to the steady state. The deformation of coated cylinders for different values of rubber shear modulus is shown in Fig. 9. Large deformation was visible in the cylinder that had a shear modulus of 95.8 psi. However, for larger values of shear modulus, the amount of deformation is small and is commensurate with deformation observed in the uncoated aluminum cylinder model. The results of this study seem to indicate that the dynamic response of the cylinder is related to the stiffness of the coating and is therefore affected by the value of the shear modulus. Furthermore, the dramatic change in the response of the cylinder due to a change in the shear modulus of the coating suggests the existence of a shear modulus "threshold" value, that is, a value below which the coated cylinder adversely responds to an underwater shock wave.

In the second case, the objective was to examine the sensitivity of the response to a change in the coefficient of asymmetry while holding the shear modulus of the rubber constant. Again, composite model 1 was utilized and the coefficient of asymmetry was varied from 0.223 to 0.750. At nearly all locations, axial and hoop strain values exhibited relatively small deviations until late time (later than 2 ms). The internal energy level of the aluminum was virtually identical for both cylinders up through 2.2 ms and then

showed a deviation thereafter. Strain results indicate that the dynamic response of the coated cylinder was less influenced by changes in the coefficient of asymmetry than changes in the shear modulus. The effect of changes in the asymmetry coefficients was not evident until late time.

In the third case, the objective was to determine how a variation in the thickness of the aluminum would affect the dynamic response of the coated cylinder. The thickness of the aluminum shell material in composite model 1 was changed from 0.250 to 0.125 in. and to 0.375 in. The thickness of the aluminum endplate remained constant (1-in. thick). The results show that the thickness variation affected the cylinder differently depending on the location where an element was analyzed. For example, away from the endplate, hoop strain values were generally higher when the aluminum thickness was reduced. However, the thinner aluminum resulted in lower axial strain values near the endplate. To gain a better perspective on what the overall effect was, effective plastic strain was plotted for elements A3 and C3 and is shown in Fig. 10 and 11. These plots showed that the thicker aluminum generally resulted in lower plastic strain at locations away from the endplate but higher plastic strain near the endplate. Aluminum deformation is shown in Fig. 12 for the three different thickness cases. Deformations were scaled by a factor of five. The deformation patterns were different for each case. The internal energy of the aluminum shell material was also plotted and is shown in Fig. 13. The results indicate that as the metal thickness was reduced, the internal energy was also reduced. Results of this study indicate that variations of metal thickness have a locally different effect on response but the total internal energy was larger for a thicker aluminum cylinder.

In the fourth case, the objective was to determine how a variation in the coating thickness would affect the dynamic response of the cylinder. The thickness of the tread stock rubber in composite model 1 was changed from 0.250 to 0.125 in. and to 0.375 in. At nearly all locations, the response of the cylinder significantly improved when the rubber thickness was increased but was adversely affected when the rubber thickness was decreased. Differences in response can be seen in the deformation of the cylinder for each case and are shown in Fig. 14. Cylinder response was also examined for a rubber thickness of 0.500 in. and it was found that the response of the cylinder improved. Internal energy of the aluminum shell material is plotted for the various rubber thicknesses and is shown

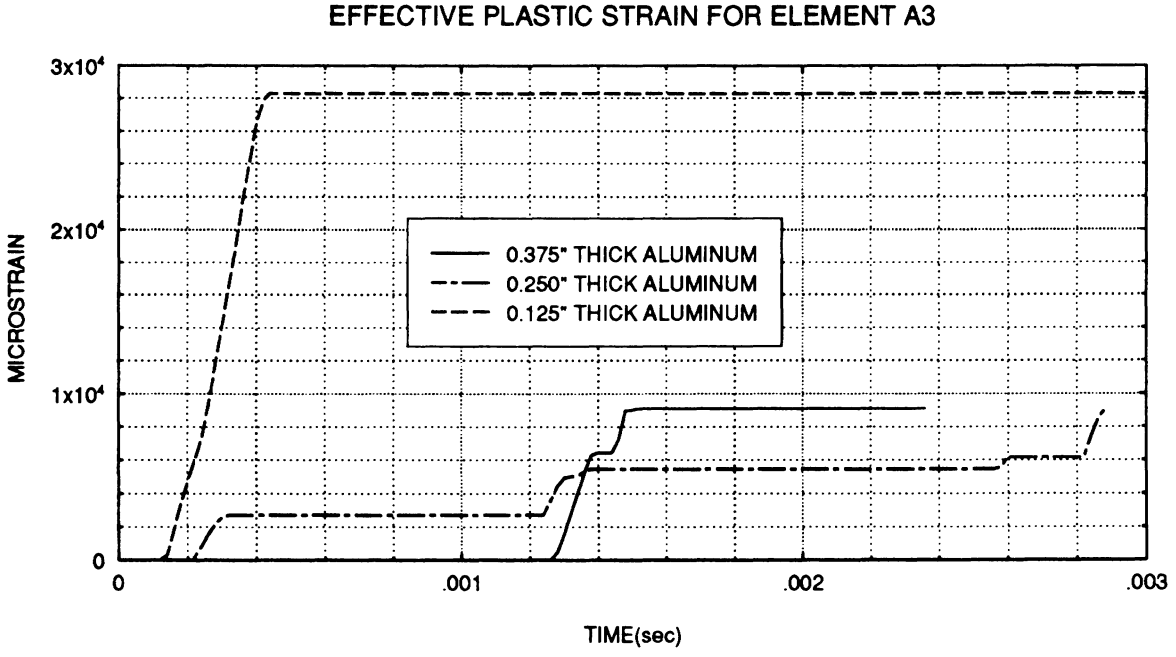

FIGURE 10 Effective plastic strain at position A3 for coated cylinders with variation of aluminum shell thickness.

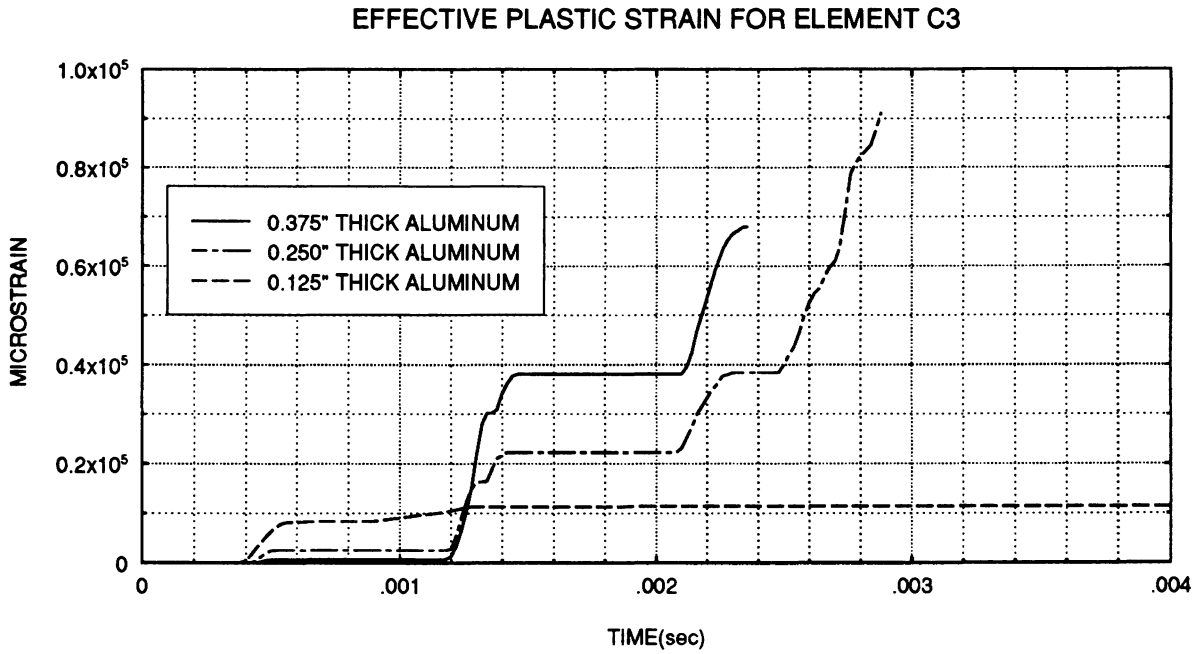

FIGURE 11 Effective plastic strain at position C3 for coated cylinders with variation of aluminum shell thickness.

in Fig. 15. Early termination of the problem in the thin rubber case was due to a severe distortion of the model mesh. As observed in the previous cases, the results of this study also support the hypothesis that the dynamic response of the cylinder is related to the stiffness of the coating and is therefore affected by the thickness of the coating. The significant difference in response due to changes in coating thickness again suggest the existence of a thickness "threshold" value,

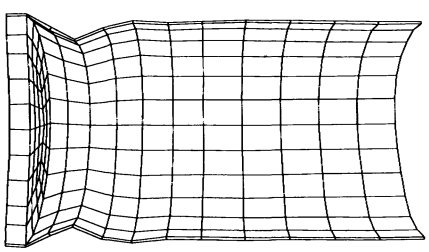

0.125" THICK ALUMINUM (DISPL. SCALE FACTOR OF 5)

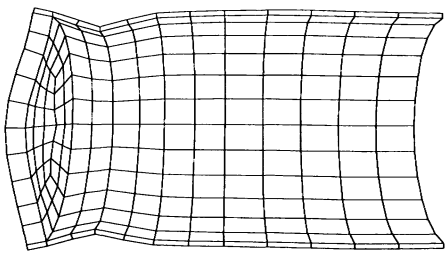

0.250" THICK ALUMINUM (DISPL. SCALE FACTOR OF 5)

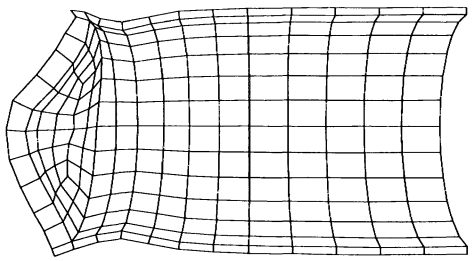

0.375" THICK ALUMINUM (DISPL. SCALE FACTOR OF 5)

FIGURE 12 Deformation of coated cylinders with variation of aluminum shell thickness at 2.34 ms.

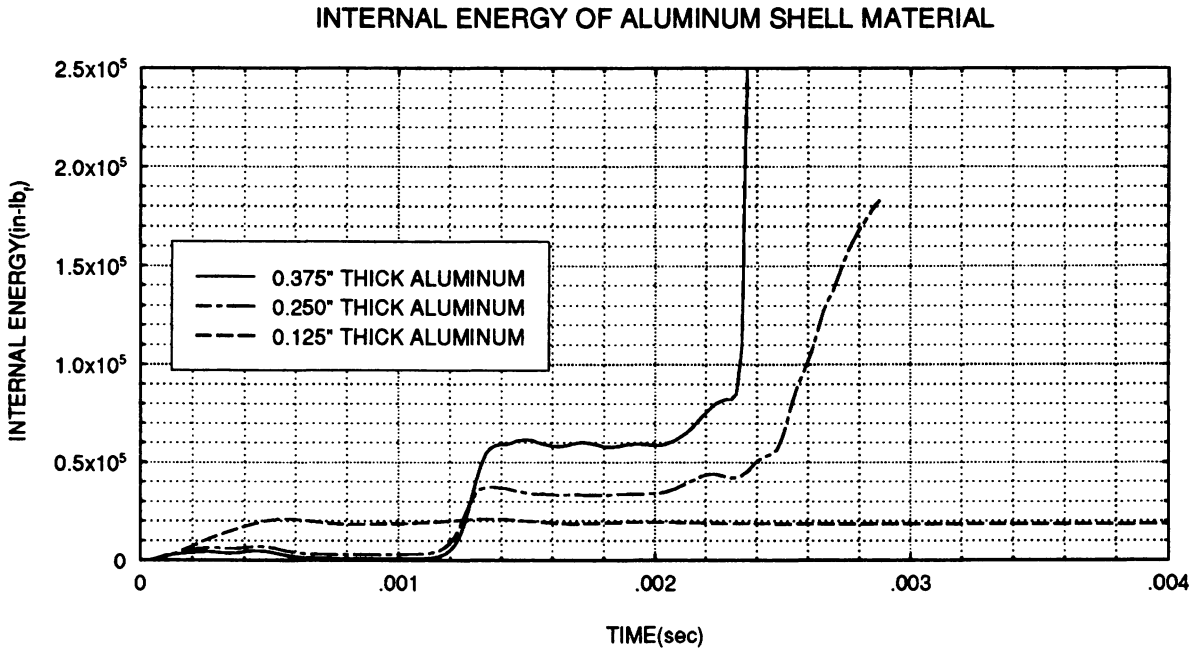

FIGURE 13 Internal energy of aluminum shell material of coated cylinders with variation of aluminum shell thickness.

that is, a value below which the coated cylinder responds adversely to an underwater shock wave.

In the last case, the objective was to determine how a change in the metal material would affect the dynamic response of the cylinder. For this study, an uncoated steel cylinder was compared to a steel cylinder coated with tread stock rubber. The steel shell thickness and coating thickness were both 0.250 in. The endplate thick-

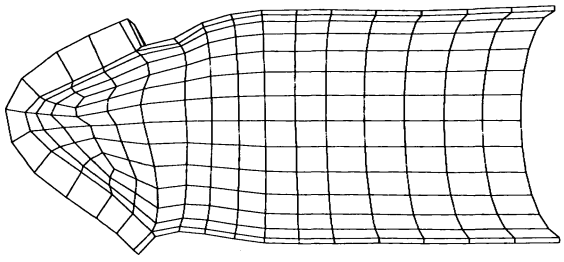

0.250" THICK RUBBER (DISPL. SCALE FACTOR OF 5)

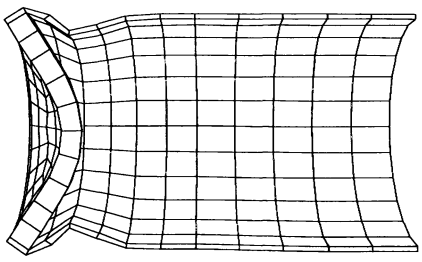

0.375" THICK RUBBER (DISPL. SCALE FACTOR OF 5)

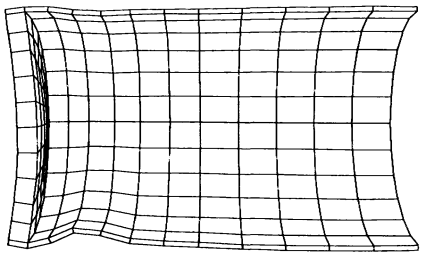

0.500" THICK RUBBER (DISPL. SCALE FACTOR OF 5)

FIGURE 14 Deformation of coated aluminum cylinders with variation of rubber thickness at 2.86 ms.

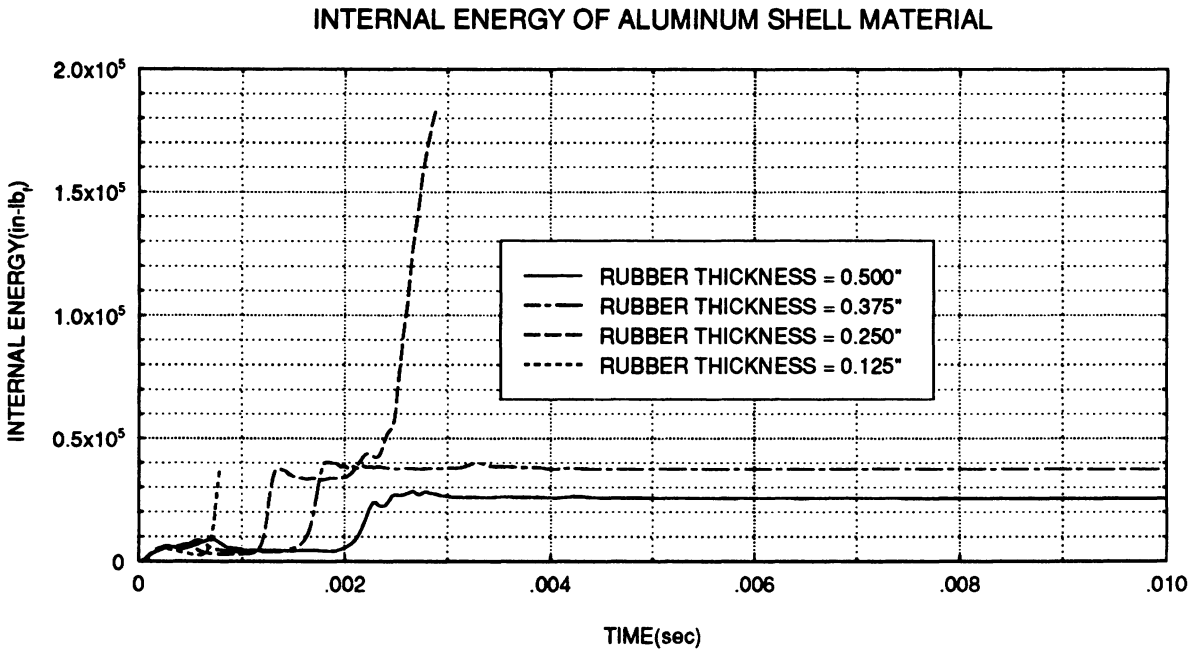

FIGURE 15 Internal energy of aluminum shell material for coated cylinders with variation of rubber thickness.

ness was 1 in. as in the aluminum cylinder cases. Results were similar to those obtained for the aluminum cylinder. Again, axial and hoop strain values were larger in the coated cylinder than in the uncoated cylinder. It was noted that the ratio of the maximum response of the coated and uncoated cylinders was generally higher in the case of steel than in the case of aluminum. For example, at location B3, for response up through 1.3 ms, the ratio of coated to uncoated maximum axial strain was 4.3 for steel and 1.8 for aluminum. This is probably attributable to the higher stiffness of steel compared to aluminum.

CONCLUSIONS

Under certain conditions, when subjected to underwater shock, surface coatings appeared to concentrate wave energy within the structure for longer duration, resulting in significantly higher magnitudes of stress and strain. Instead of a gradual release of energy into the surrounding water medium, most of the energy was retained in the metal material. Cylinder response was most influenced by changes in rubber shear modulus and rubber thickness. Increasing these values resulted in improved cylinder response. Both parameters are related to the coating stiffness and it is this property that most likely governs the extent of the energy transfer in the structure and the surrounding water medium, and consequently the dynamic response of the cylinder. Results point to the existence of threshold values for both coating shear modulus and coating thickness, values below which lead to adverse and erratic cylinder response.

REFERENCES

Banerjee, P. K., and Butterfield, R., 1981, *Boundary Element Methods in Engineering Science,* McGraw–Hill, London.

Chisum, J. E., 1992, "Response Predictions for Double Hull Cylinders Subjected to Underwater Shock Loading," Master's Thesis, Naval Postgraduate School, Monterey, CA.

DeRuntz, J. A., Jr., 1989, "The Underwater Shock Analysis Code and its Applications," *60th Shock and Vibration Symposium,* Virginia Beach, VA.

Fox, P. K., Kwon, Y. W., and Shin, Y. S., 1992, "Nonlinear Response of Cylindrical Shells to Underwater Explosion: Testings and Numerical Prediction Using USA/DYNA3D," Report NPS-ME-92-002, Naval Postgraduate School, Monterey, CA, March.

Geers, T. L., 1971, "Residual Potential and Approximate Methods for Three Dimensional Fluid–Structure Interaction Problems," *Journal of the Acoustical Society of America,* Vol. 49, pp. 1505–1510.

Geers, T. L., 1975, "Shock-Wave Attenuation by Resilient Scatterers," *Journal of Applied Mechanics,* Vol. 42, pp. 390–394.

Geers, T. L., 1978, "Doubly Asymptotic Approximations for Transient Motions of Submerged Structures," *Journal of the Acoustical Society of America,* Vol. 64, pp. 1500–1508.

Mooney, M., 1940, "A Theory of Large Elastic Deformation," *Journal of Applied Physics,* Vol. 11, pp. 582–592.

Nelson, K. W., Shin, Y. S., and Kwon, K. W., 1992, "Failure of Aluminum Cylinder From Underwater Shock Effects," *63rd Shock & Vibration Symposium,* Las Cruces, NM, October, pp. 83–95.

Park, K. C., Felippa, C. A., and DeRuntz, J. A., 1977, "Stabilization of Staggered Solution Procedures for Fluid–Structure Interaction Analysis," *Computational Methods for Fluid Structure Interaction Problems,* in T. Belytschko, and T. L. Geers, Eds., AMD-Vol. 26, ASME, pp. 95–124.

Stillman, D. W., and Hallquist, J. O., 1990, "VEC/DYNA3D User's Manual (Nonlinear Dynamic Analysis of Structures in Three Dimensions)," Livermore Software Technology Corporation Report 1018, June.